

Stochastic realization shift in the ground-state hyperfine transition of an alkali-metal vapor

J. C. Camparo

Mail Stop M2-253, Electronics Technology Center, The Aerospace Corporation, P.O. Box 92957, Los Angeles, California 90009

(Received 16 February 1996)

Several years ago, a resonance-shift phenomenon was predicted to exist, termed the stochastic realization shift (SRS), which arises as a consequence of correlated amplitude and frequency variations in a resonant field. An interesting aspect of the phenomenon is that the sign of the SRS in weak and strong fields has been shown to differ. Here, we demonstrate that the SRS may be conveniently studied over a broad range of field strengths via magnetic resonance in an optically pumped alkali-metal vapor. Specifically, we study the SRS in the ground state 0-0 hyperfine transition of Rb^{87} for a field undergoing stochastic (yet correlated) amplitude-frequency fluctuations. Under our experimental conditions we find no evidence for a change in sign of the SRS as the field strength undergoes a transition from weak to strong. Further, our results show that in strong fields the magnitude of the SRS may be influenced by the field's spatial variations. [S1050-2947(96)07307-6]

PACS number(s): 32.70.Jz, 32.80.Bx, 32.30.Bv

I. INTRODUCTION

During the course of some Monte Carlo studies examining ac Stark shifts induced by stochastic fields, Camparo and Lambropoulos [1,2] found that a finite realization of a fluctuating-field-atom interaction always gives rise to a shift in the observed resonance frequency. Since their explanation for the shift appealed to the fact that any finite realization of a stochastic process violates the ergodic theorem, they termed this phenomenon the stochastic realization shift (SRS). The effect, however, is more than a statistical artifact as its name might imply, since the shift will persist even for an infinite realization of a stochastic process if the field suffers correlated amplitude and frequency variations. Evidence for these theoretical claims first came from magnetic-resonance experiments performed by Camparo and Klimcak [3], where a resonant microwave field was subject to sinusoidal (as opposed to stochastic) amplitude and frequency modulation. Later, van Exter *et al.* [4] were able to demonstrate in an optical transition that the shift persists even if the correlated amplitude and frequency variations are stochastic in nature.

In the regime of weak fields, where resonance is often operationally defined as the field frequency that maximizes the atomic excitation rate, the SRS may be conveniently interpreted in terms of a convolution between the field spectrum and the atomic absorption cross section. From first-order perturbation theory it can be shown that the excitation rate Γ for an atom interacting with a broad band field is given by [5]

$$\Gamma(\omega_f) = \int_{-\infty}^{\infty} S(\omega - \omega_f) \sigma(\omega - \omega_a) d\omega. \quad (1)$$

Here, $S(\omega - \omega_f)$ is the spectral density of the field, the peak of which occurs at a frequency ω_f , while $\sigma(\omega - \omega_a)$ is the absorption cross section of the atom at frequency ω with ω_a the atom's unperturbed resonance frequency. For a field with positive (negative) correlation between its amplitude and frequency variations, $S(\omega - \omega_f)$ will be an asymmetric function with a tail extending to high (low) Fourier frequen-

cies. Consequently, the convolution will be maximized for $\omega_f < \omega_a$ ($\omega_f > \omega_a$), giving rise to a negative (positive) shift in the observed atomic resonance frequency.

In strong fields, first-order perturbation theory no longer applies and the convolution model breaks down. Specifically, not only is the convolution model incapable of predicting the correct magnitude for the SRS in strong fields, it cannot be trusted to predict the correct sign for the SRS [3]. Yet many spectroscopic experiments require moderate to strong fields, and some quantum electronics devices such as atomic clocks operate just at saturation of an atomic transition. There is, therefore, strong motivation for studying the SRS in the moderate- to strong-field regime. Unfortunately, optical SRS experiments in the strong-field regime are not without difficulty. First, there is the issue of Doppler broadening. If this is not eliminated in some fashion, either through the use of sub-Doppler spectroscopic techniques or atomic beams, then a straightforward interpretation of the SRS data could require power broadening of the entire Doppler line shape. Moreover, optical pumping effects cannot be ignored in the strong-field regime, as these can lead to line shape distortions [6]. Finally, the generation of strong optical fields with well controlled stochastic characteristics is a nontrivial laboratory challenge [7].

In this work we demonstrate that these experimental difficulties may be avoided by studying the SRS using magnetic resonance in an optically pumped alkali-metal vapor. The specific advantages to this approach are (i) the relative ease of creating strong rf or microwave fields with well defined stochastic characteristics, (ii) the fact that optical pumping does not confound an interpretation of the observed shift, and (iii) the elimination of Doppler broadening as a consequence of Dicke narrowing [8]. We demonstrate the approach by studying an SRS in the 0-0 hyperfine transition of Rb^{87} , which has application to atomic-clock technology.

Based on previous investigations, we expected the SRS to change sign as the field strength underwent a transition from weak to strong. As we will show, however, this was not observed under our experimental conditions. Further, we will show that a density-matrix computation of the SRS (no free parameters) is in good agreement with experiment except in

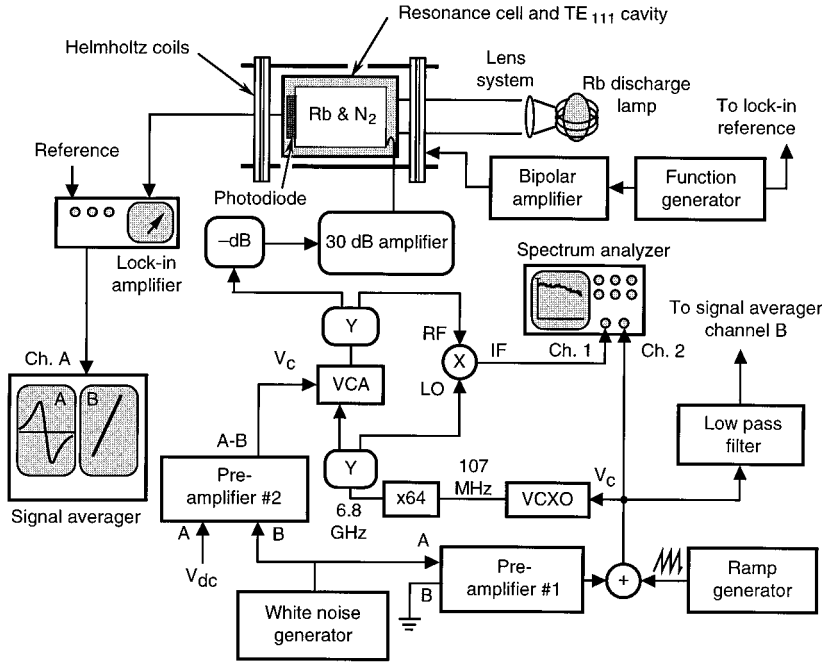


FIG. 1. Optical-pumping magnetic-resonance experimental arrangement described in the text.

the regime of very strong fields. Although the sign of the theoretical shift is consistent with experiment over all field strengths, the magnitude of the SRS is not. To explain the discrepancy we hypothesize that the strong field SRS is sensitive to the field's spatial variations, since these are not included in the density-matrix computation.

II. EXPERIMENT

The experiment employed a standard optical-pumping/magnetic-resonance arrangement as illustrated in Fig. 1 [9]. A pyrex resonance cell containing natural Rb (i.e., 72% Rb^{85} and 28% Rb^{87}) and 10 torr of N_2 was placed in a microwave cavity whose TE_{111} mode was resonant with the ($F=2, m_F=0$) - ($1,0$) ground-state hyperfine transition of Rb^{87} (see Fig. 2). Braided windings wrapped around the cylindrical cavity heated the resonance cell to $\sim 70^\circ\text{C}$ (i.e., $[\text{Rb}] \approx 1.2 \times 10^{12} \text{ cm}^3$) [10], and the entire assembly was centrally located in a Helmholtz coil pair. Light from an isotopically enriched Rb rf-discharge lamp optically pumped the alkali vapor, providing a population imbalance between the two $m_F=0$ sublevels of the Rb^{87} ground state, and the transmission of this lamp light through the vapor was monitored with a photodiode placed inside the microwave cavity.

As a consequence of optical pumping, light transmission through the vapor is relatively high in the absence of resonant microwaves. However, if the microwave field in the cavity is resonant with the Rb^{87} 0-0 hyperfine transition, the degree of optical pumping is reduced and so is the level of lamp light transmitted by the vapor. Thus, the 0-0 hyperfine transition line shape may be observed in the photodiode output by sweeping the microwave frequency across the 0-0 hyperfine resonance. In the present experiment, the magnetic field provided by the Helmholtz coils was sinusoidally modulated at 97.3 Hz about its average value B_0 (i.e., $B_0 = 3.4 \text{ G}$ and $B_{p-p} = 0.064 \text{ G}$), resulting in a sinusoidal modulation of the 0-0 hyperfine transition frequency as a

consequence of the transition's second-order Zeeman shift [11]. A signal proportional to the transition's derivative was obtained by employing phase-sensitive detection, and the signal's zero crossing could be used to measure the 0-0 hyperfine transition's resonant frequency.

The microwaves were derived from a voltage-controlled crystal oscillator (VCXO), which had a modulation bandwidth of 10 KHz [12], and whose output at $\sim 107 \text{ MHz}$ was multiplied up into the gigahertz regime before being amplified by a 30-dB solid-state amplifier. The microwave power entering the cavity could be controlled with variable attenuators (labeled as -dB in Fig. 1), and these were calibrated to microwave Rabi frequency Ω by measuring the linewidth of

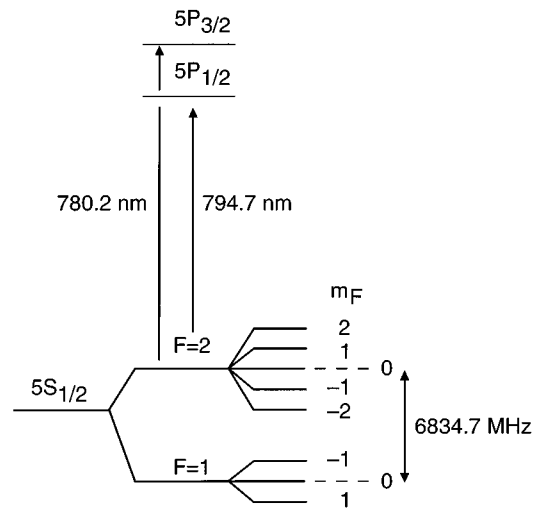


FIG. 2. Relevant energy-level diagram of Rb^{87} . In thermal equilibrium all Zeeman sublevels of the ground state are equally populated. However, optical excitation of one hyperfine manifold of Zeeman states (e.g., the $F=2$ manifold) by D_1 (794.7 nm) and/or D_2 (780.2 nm) light will optically pump atoms into the nonabsorbing hyperfine manifold.

the hyperfine transition in the absence of noise [13]. Extrapolating the linewidth measurements to zero microwave power indicated that the intrinsic dephasing rate in our system, γ_2 , was 230 Hz.

The white-noise output from a commercial synthesized function generator (bandwidth limited at 15 MHz) was split and passed to two preamplifiers. Preamplifier No. 1 had a pass band of $0.1\text{--}10^6$ Hz (roll-off 6 dB per octave), and its output was used to generate VCXO frequency fluctuations. Preamplifier No. 1's output noise voltage was measured with a spectrum analyzer, and from those measurements, along with the transfer function of the VCXO (i.e., $|H(f)|^2 \cong k\gamma_{\text{VCXO}}^2/(\gamma_{\text{VCXO}}^2 + f^2)$, where $k = -50.82$ KHz per volt and $\gamma_{\text{VCXO}} = 10$ KHz), we could infer that the 6834.7-MHz microwaves experienced bandwidth limited frequency fluctuations, $\delta\omega$, with a standard deviation of 1.7 KHz. Preamplifier No. 2 had a pass band from dc to ν_{high} (maximum value of $\nu_{\text{high}} = 300$ KHz and a roll-off of 6 dB per octave), and its output provided the control voltage V_c for a voltage-controlled attenuator (VCA). (The VCA was a modular, commercial device with a linear transfer function of -4 dB per volt and a bandwidth on the order of 10^5 Hz.) Since the noise had a mean of zero, it needed to be added to some fixed dc voltage for input to the VCA. By mixing the microwave signal just prior to and just after the VCA, we could measure the relative amplitude noise $\delta\epsilon$ of the microwave signal. (This measurement was accomplished with both of preamplifier No. 1's inputs grounded.) For the two experiments to be described subsequently, the standard deviation of the relative amplitude noise, $\sigma_{\delta\epsilon}$, was 0.37 and 0.29, respectively, for $\nu_{\text{high}} = 10^5$ Hz. Note that since the amplitude and frequency noise of the field were derived from the same white-noise generator, they were highly correlated though stochastic.

Using the above measured values for the field's amplitude and frequency noise, we numerically simulated a realization of the stochastic microwave field for the case of positively correlated amplitude-frequency fluctuations [14]. Fourier transformation of the field's autocorrelation function then yielded the simulated microwave field's spectrum, and this is shown in Fig. 3(a). The spectrum appears nearly Lorentzian with a linewidth (full width at half maximum) $2\gamma_f$ of 620 Hz. In combination with our estimation of γ_2 , this would imply that the actual atomic dephasing rate in these experiments, Γ , was about 540 Hz ($\Gamma \cong \gamma_2 + \gamma_f$) [15]. However, as illustrated in Fig. 3(b), which shows the difference between our simulated field spectrum and a Lorentzian, the microwave field had a slight asymmetry to high Fourier frequencies, as expected for a field exhibiting positively correlated amplitude-frequency fluctuations.

The experiment was performed by slowly sweeping the microwave frequency across the 0-0 hyperfine resonance and recording the output of the lock-in amplifier with a signal averager. Simultaneously, the signal averager also recorded the ramp voltage applied to the VCXO. Several hundred sweeps across resonance were averaged in order to improve the signal-to-noise ratio, and the ramp voltage corresponding to the averaged signal's zero crossing was taken as a measure of the resonance frequency. For given Ω and ν_{high} , two measurements were performed corresponding to $\langle\delta\omega\delta\epsilon\rangle = \text{positive}$ and $\langle\delta\omega\delta\epsilon\rangle = \text{negative}$. The change from positive

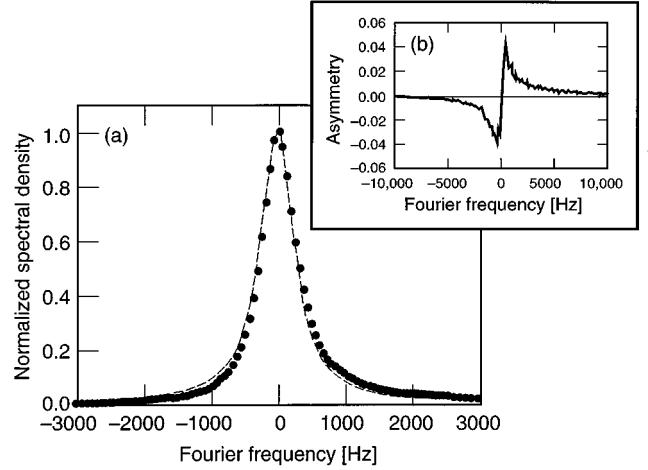


FIG. 3. (a) Computationally simulated spectrum of the experiment's stochastic microwave field (filled circles) along with a Lorentzian approximation (dashed line). (b) Asymmetry of the microwave field determined by taking the difference between the computed spectrum and the Lorentzian approximation.

to negative correlation could be performed easily by inverting the output of preamplifier No. 1. Defining $\omega_+(\omega_-)$ as the resonance frequency for positively (negatively) correlated amplitude-frequency fluctuations, the SRS = $(\omega_+ - \omega_-)/2$. For fixed conditions, the results to be presented below represent averages of several SRS measurements made in this way.

III. RESULTS

A. SRS dependence on the amplitude-frequency covariance

Given the transfer functions of the VCXO and preamplifier No. 2, it is straightforward to show that the covariance of $\delta\omega$ and $\delta\epsilon$ has a fairly simple expression:

$$\langle\delta\omega\delta\epsilon\rangle \equiv \langle\delta\omega(t)\delta\epsilon(t)\rangle = \frac{A\nu_{\text{high}}\gamma_{\text{VCXO}}}{\nu_{\text{high}} + \gamma_{\text{VCXO}}}, \quad (2)$$

where A is a proportionality constant. Thus, the strength of the amplitude-frequency correlation could be easily altered by varying ν_{high} , and our results examining the SRS as a function of ν_{high} are shown by the filled black circles in Fig. 4 for the case of a moderately strong field (i.e., $\Omega = 525$ Hz and $\sigma_{\delta\epsilon} = 0.37$). Since $\Omega \cong \Gamma$, this field strength corresponded to the onset of saturation. As a check of our ability to measure an SRS, the noise input to preamplifier No. 2 was grounded with $\nu_{\text{high}} = 300$ KHz, and the resulting shift is shown by the filled gray circle in Fig. 4 (i.e., without amplitude noise there is no frequency shift).

van Exter *et al.* [4] have argued that in weak fields the stochastic realization shift arises because the “intensity-weighted” average frequency of a field is not necessarily equivalent to the “cycle-averaged” field frequency. Consequently, in weak fields one expects the SRS to be proportional to the amplitude-frequency covariance: SRS (weak-field) $\sim -\langle\delta\omega\delta\epsilon\rangle$. In strong fields, Camparo and Lambropoulos [1] have shown that the SRS should also be proportional to the amplitude-frequency covariance, but with the opposite sign: SRS (strong-field) $\sim \langle\delta\omega\delta\epsilon\rangle$. The solid

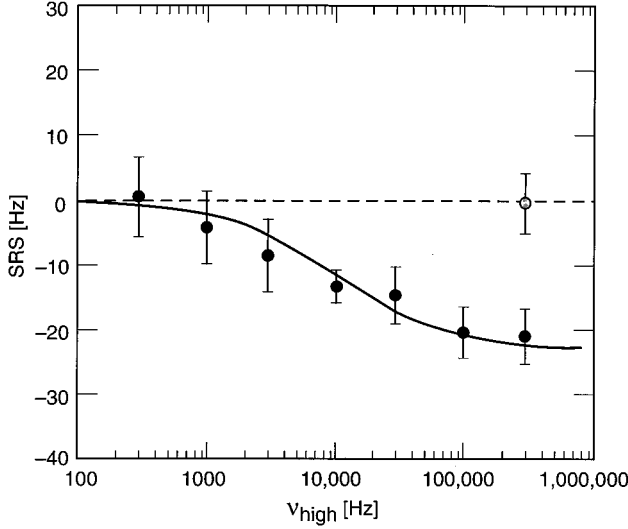


FIG. 4. The SRS as a function of preamplifier No. 2's high-frequency roll-off, ν_{high} (i.e., $\langle \delta\omega \delta\epsilon \rangle$). Filled black circles correspond to the measurements, while the filled gray circle corresponds to an SRS measurement without amplitude noise. The solid line is a fit of the data to Eq. (2).

line in Fig. 4 is a fit to the data using Eq. (2) with the constant A as a free parameter. The agreement between Eq. (2) and our experimental data clearly indicates a proportionality between the SRS and $\langle \delta\omega \delta\epsilon \rangle$ in the intermediate-field-strength regime.

B. SRS dependence on the Rabi frequency

Our primary motivation for initiating these studies was to investigate the SRS as a function of Rabi frequency. The results of those measurements are shown as filled black circles in Fig. 5 (i.e., $\nu_{\text{high}} = 100$ KHz and $\sigma_{\delta\epsilon} = 0.29$). As expected, in weak fields the SRS was negative. However, the SRS remained negative even when the field strength was quite strong, i.e., Rabi frequencies roughly five to six times

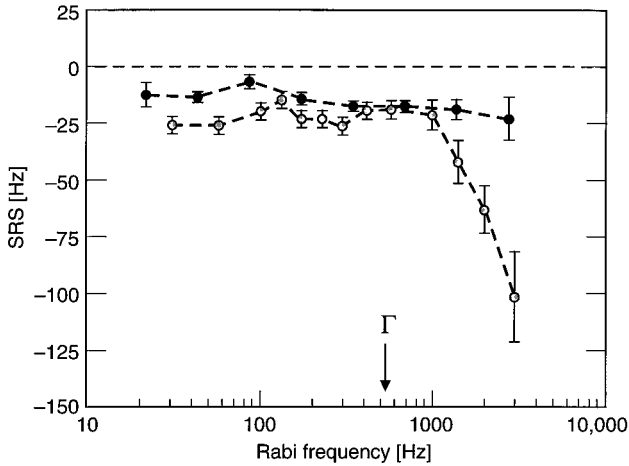


FIG. 5. The SRS as a function of Rabi frequency. The atomic dephasing rate in the experiments, including field bandwidth, is denoted by Γ . Filled black circles correspond to the experimental results. Filled gray circles correspond to the results from Monte Carlo simulation.

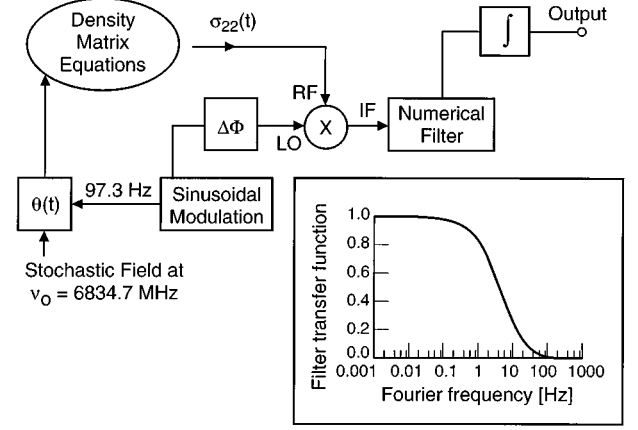


FIG. 6. Schematic of the computational procedure used to calculate an SRS as described in the text.

larger than Γ . Moreover, the magnitude of the SRS was approximately constant over the entire range of field strengths that were investigated. These observations are qualitatively different from those of Ref. [3], where the SRS was examined as a function of Rabi frequency for a field with *deterministic* amplitude-frequency variations. This difference prompted a Monte Carlo density-matrix investigation of the SRS corresponding to our experimental conditions.

Figure 6 shows a schematic of the experiment from a computational perspective. The phase (i.e., frequency) of a resonant, stochastic microwave field is sinusoidally modulated, thereby creating a corresponding modulation in the population density of the two states coupled by the field. The oscillating population density at each instant of time is multiplied by the original phase-modulation signal with a suitable phase delay, $\Delta\Phi$ [16]; the mixer output is numerically filtered in order to eliminate harmonics, and the filter output is integrated. Resonance is defined as the microwave frequency that zeros the integrator output.

The oscillating population density was computed via the two-level density matrix equations [17]:

$$\frac{d\sigma_{22}}{dt} = \gamma_1(\sigma_{22}^{\text{eq}} - \sigma_{22}) + [\Omega + \delta\Omega(t)]\text{Re}[ie^{-i\theta(t)}\sigma_{12}^*], \quad (3a)$$

$$\left\{ \frac{d}{dt} - i[\Delta_0 + \delta\omega(t)] + \gamma_2 \right\} \sigma_{12} = \frac{i[\Omega + \delta\Omega(t)]}{2} e^{-i\theta(t)} (1 - 2\sigma_{22}). \quad (3b)$$

Here, Δ_0 is the detuning of the field from the unperturbed atomic resonance; σ_{22} is the population density in the upper level with a value of σ_{22}^{eq} in the absence of the field; σ_{12} is the coherence; $\delta\omega$ and $\delta\Omega$ are stochastic fluctuations in the field frequency and the Rabi frequency, respectively; $\theta(t)$ is the sinusoidally modulated phase of the stochastic field, and for the present experiment we had $\gamma_1 = \gamma_2$. [In deriving Eqs. (3), normalization is assumed: $\sigma_{11} + \sigma_{22} = 1$.] It should be noted that the above density-matrix equations do not include

any macroscopic effects (e.g., variations of the magnetic, microwave or optical fields over the resonance cell volume) [18]. For a single realization of the dynamics, the density-matrix equations were solved with a variable step-size, fourth-order Runge-Kutta algorithm [19] and in order to eliminate the significance of transient effects on the SRS the integrator output was examined from $t=0.5$ to $(2.5\pm 10\%)$ s (note that $\gamma_2^{-1}\cong 0.005$ s). (The final time was randomized in order to avoid potential aliasing effects arising from the deterministic modulation.)

The filled gray circles in Fig. 5 correspond to the computational results with no free parameters. Consistent with experiment, the computation predicts that there should be no change in sign of the shift over the field strengths investigated in our experiments. Although we do not yet have a clear qualitative understanding of why these results differ from those of Ref. [3], two possible explanations may be presented. It might be that our experiment did not achieve the required microwave power levels necessary to observe a change in sign of the SRS [20]. Alternatively, it might be that constancy in the sign of the SRS is a basic consequence of the amplitude-frequency variations's stochastic nature.

In weak to moderately strong fields, the agreement between computation and experiment is good. In particular, both computation and experiment suggest a slight "dip" in the magnitude of the SRS for $\Omega \sim 100$ Hz. In strong fields (i.e., $\Omega > \Gamma$), the results from computation and experiment diverge. Although our computations indicate that the probability distribution for the SRS is asymmetric (i.e., $|\text{mean SRS}| > |\text{modal SRS}|$), this alone cannot account for the discrepancy. As we discuss below, it is believed that spatial variations in the microwave field can play an important role in determining an SRS.

We note that the resonant mode of our microwave cavity was a TE_{111} mode, whose magnetic field z component has a node along the cavity axis. This component of the microwave field drives the 0-0 hyperfine transition in the alkali (i.e., the z axis corresponds to the cavity axis, and is also the atomic quantization axis). Due to the presence of the N_2 buffer gas in the resonance cell, the Rb atoms were "frozen" in place on the time scale of the Rabi period [21]. Thus, the observed signal was essentially a sum of atomic signals from groups of atoms that experienced different microwave field strengths corresponding to their position in the cavity: atoms near the cavity axis experienced weak microwave fields, while atoms further away from the cavity axis experienced stronger microwave fields. Given a spatially inhomogeneous field, and a relative immobility of atoms, it has been shown that the central portion of an observed line shape will be dominated by those groups of atoms that experience field

strengths corresponding to the onset of saturation [22]. Thus, even though the average Rabi frequency experienced by the sample of atoms increased in the experiment, line center (and hence an SRS) would have been determined by the relatively constant Rabi frequency corresponding to the onset of saturation. In the computations no account was taken of the microwave field's spatial mode, so that beyond saturation one might expect the experimental SRS values (black circles in Fig. 5) and the computational SRS values (gray circles) to diverge. Note also that this reasoning would imply a constancy in the sign of the shift as well as magnitude, even if computation predicted a sign change for the SRS at Rabi frequencies higher than those studied here. If the field's spatial mode is important in determining an SRS, then performing the experiment with a TE_{011} mode cavity, whose microwave field z component is maximized along the cavity axis, would yield strong-field SRS data in better agreement with computation. (The experiment should be performed with a coated resonance cell that does not contain a buffer gas [23] and/or a diode laser should be employed in place of the lamp so that only the central portion of the cavity mode is probed [24].)

IV. SUMMARY

In this work we have demonstrated that stochastic realization shifts may be conveniently studied in optical-pumping magnetic-resonance experiments with alkali vapors. Specifically, we have studied the SRS in the ground-state hyperfine transition of Rb^{87} , which has application to atomic-clock technology. We have investigated the SRS as a function of Rabi frequency, finding no evidence of a change in sign of the SRS as the field strength changed from weak to strong. This result differs qualitatively from that of Ref. [3] and might be due to the limited magnitude of the Rabi frequency that could be achieved in the present experiments. Alternatively, the constancy in sign of the SRS could be a more general result associated with the stochastic nature of the resonant field. The experimental dependence of the SRS on Rabi frequency was found to agree quite well with a density-matrix computation of the shift except in very strong fields, where we hypothesize that the discrepancy is a consequence of the stochastic field's spatial distribution.

ACKNOWLEDGMENTS

The author would like to express his gratitude to Dr. B. Jadaszliwer for a critical reading of the manuscript. This work was supported by the Aerospace Corporation's Aerospace Sponsored Research program.

-
- [1] J.C. Camparo and P. Lambropoulos, *Opt. Commun.* **85**, 213 (1991).
 - [2] J.C. Camparo and P. Lambropoulos, *J. Opt. Soc. Am. B* **9**, 2163 (1992).
 - [3] J.C. Camparo and C.M. Klimcak, *Opt. Commun.* **91**, 343 (1992).

- [4] M.P. van Exter, D.M. Boersma, A.K. Jansen van Doorn, and J.P. Woerdman, *Phys. Rev. A* **49**, 2861 (1994).
- [5] For an outline of how this is accomplished, see A.M. Bonch-Bruевич and V.A. Khodovoi, *Sov. Phys. Uspekhi* **8**, 1 (1965).
- [6] See, for examples, R. Walkup, A. Spielfiedel, W.D. Phillips, and D. Pritchard, *Phys. Rev. A* **23**, 1869 (1981); J.E.

- Bjorkholm, P.F. Liao, and A. Wakaun, Phys. Rev. A. **26**, 2643 (1982); C.M. Klimcak and J.C. Camparo, *ibid.* **30**, 1791 (1984).
- [7] D.S. Elliot and S.J. Smith, J. Opt. Soc. Am. **5**, 1927 (1988); C. Xie, G. Klimeck, and D.S. Elliot, Phys. Rev. A **41**, 6376 (1990).
- [8] R.H. Dicke, Phys. Rev. **89**, 472 (1953).
- [9] L.C. Balling, in *Advances in Quantum Electronics*, edited by D.W. Goodwin (Academic, London, 1975), pp. 1–167.
- [10] T.J. Killian, Phys. Rev. **27**, 578 (1926).
- [11] A. Corney, *Atomic and Laser Spectroscopy* (Clarendon, Oxford, 1977), Chap. 18.
- [12] For a brief discussion of VCXO characteristics, see R.L. Kent (unpublished).
- [13] J.C. Camparo and R.P. Frueholz, Phys. Rev. A **31**, 1440 (1985); **32**, 1888 (1985).
- [14] J.C. Camparo and P. Lambropoulos, Phys. Rev. A **47**, 480 (1993).
- [15] A.T. Georges and P. Lambropoulos, Phys. Rev. A **18**, 587 (1978).
- [16] J.C. Camparo and R.P. Frueholz, in *Proceedings of the 1993 IEEE International Frequency Control Symposium* (IEEE, New York, 1993), p. 114.
- [17] For a further discussion of the solution of the density-matrix equations under fluctuating field conditions, see R.P. Frueholz and J.C. Camparo, Phys. Rev. A **47**, 4404 (1993); **52**, 472 (1995); and Ref. [14].
- [18] J.C. Camparo, in *Frequency Standards and Metrology* (Springer-Verlag, Berlin, 1989), p. 62.
- [19] W. Cheney and D. Kincaid, *Numerical Mathematics and Computing* (Brooks/Cole, Monterey, 1985).
- [20] Due to the Monte Carlo nature of our computation and the increasing length of time required to integrate the density-matrix equations for increasing Rabi frequency, it was impractical to computationally investigate Rabi frequencies in excess of ~ 3 KHz.
- [21] R.P. Frueholz and J.C. Camparo, J. Appl. Phys. **57**, 704 (1985).
- [22] J.C. Camparo, Phys. Rev. A **39**, 69 (1989).
- [23] C. Rahman and H.G. Robinson, IEEE J. Quantum Electron. **QE-23**, 452 (1987).
- [24] J.C. Camparo, Contemp. Phys. **26**, 443 (1985); C.E. Wieman and L. Holberg, Rev. Sci. Instrum. **62**, 1 (1991).